Density Functional Theory Study of the Mechanism of the BF_3-Catalyzed Rearrangement of 2,3,3-Trimethyl-1,2-epoxybutane to 2,3,3-Trimethylbutanal

James M. Coxon* and Aaron J. Thorpe

Department of Chemistry, University of Canterbury, Christchurch, New Zealand

J.Coxon@chem.canterbury.ac.nz

Received April 18, 2000

The potential energy surface for the rearrangement of BF_3-coordinated 2,3,3-trimethyl-1,2-epoxybutane to 2,3,3-trimethylbutanal has been investigated at the B3LYP/6-31G* level of theory. SCRF(SCI-PCM) solvent calculations and theoretical primary and secondary kinetic isotope effects at the same level of theory provide support for a two-step process with ring opening of the BF_3-coordinated epoxide to a tertiary carbocation intermediate followed by hydride/deuteride migration to give aldehyde. The experimentally measured primary isotope effect (k_H^H/k_D^H) requires a correction for an appropriate secondary isotope effect to give a true isotope effect k_H^H/k_D^H. For the lowest energy pathway for hydride migration, the calculated secondary kinetic isotope effect is 0.92, which when applied to the experimentally measured isotope effect of $k_H^D/k_D^H = 1.73$ gives a revised "true" primary kinetic isotope effect of $k_H^H/k_D^H = 1.59$. This compares with a calculated value of 2.01. From intermediate **15**, migration of the C1−H_a proton via **19** is energetically favored over C1−H_b migration via **18** and this result is consistent with the experimental results in which hydride migration of the proton cis to the methyl is favored.

Introduction

Some years ago, we established that in the acid-catalyzed rearrangement of an unsymmetrical 1,1-disubstituted epoxide to aldehyde there was marked stereoselection in the 1,2-hydride shift of one of the prochiral hydrogens. This stereoselection was first observed for the boron trifluoride-catalyzed rearrangement of 2,3,3-trimethyl-1,2-epoxybutane[1] and is now known to be general.[2] For epoxide **1** and **2**, the ratio of deuteride/hydride migration, that is, **3**/**4**, was 2.65:1 (standard deviation 0.08)[3] and 0.89:1 (standard deviation 0.03), respectively (Figure 1). After taking into account the inherent kinetic preference for hydride to migrate in preference to deuteride, the experiment shows that there is therefore a marked inherent preference for the migration of the group, hydrogen or deuterium, cis to the methyl group.[1]

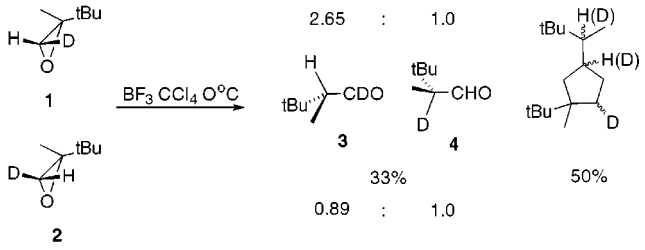

Figure 1. Rearrangement of (*Z*)- and (*E*)-1D-2,3,3-trimethyl-1,2-epoxybutanes.

It is known that the reaction occurs, at least in large measure, via the intermediacy of a discrete carbocation intermediate. This follows from the formation of both axial and equatorial aldehydes from the rearrangement of epimeric exocyclic epoxides.[4] For the reaction of 2,3,3-trimethyl-1,2-epoxybutane (**5**) with BF_3, the epoxide first coordinates with the Lewis acid (Figure 2). This is followed by cleavage of the more substituted C−O bond with consequent or subsequent rotation about the C−C bond of the epoxide and formation of a tertiary carbocation. The direction of rotation is considered to be controlled by the nonbonded interaction between the larger *tert*-butyl (cf. methyl) and solvated OBF_3^- groups, resulting in the preferential formation of conformer **6** of the carbocation where H_b is favorably oriented for migration. The model developed to understand the stereoselectivity also requires the establishment of an equilibrium ($k = k^{-1}$ with $K = 1$) between the mirror image conformers **6** and **7** with H_a migration occurring from the

* To whom correspondence should be addressed. Fax: 64 3 3642110.

(1) Blackett, B. N.; Coxon, J. M.; Hartshorn, M. P.; Richards, K. E. *J. Am. Chem. Soc.* **1970**, *92*, 2574. Blackett, B. N.; Coxon, J. M.; Hartshorn, M. P.; Richards, K. E. *Aust. J. Chem.* **1970**, *23*, 839.

(2) Blackett, B. N.; Coxon, J. M.; Hartshorn, M. P.; Richards, K. E. *Aust. J. Chem.* **1970**, *23*, 2077. Coxon, J. M.; Lim, C.-E. *Aust. J. Chem.* **1977**, *30*, 1137. Coxon, J. M.; McDonald, D. Q. *Tetrahedron Lett.* **1988**, *29*, 2575.

(3) Reaction of each epoxide, **1** and **2**, with boron trifluoride in carbon tetrachloride at 0 °C gave the aldehydes **3** and **4** and dioxolanes (50%). The isotope effect for reaction of aldehyde with epoxide will be small. ^{18}O studies show that the mechanism of dioxolane formation involves attack of a carbonyl on the epoxide and not the reverse: Blackett, B. N.; Coxon, J. M.; Hartshorn, M. P.; Lewis, A. J.; Little, G. R.; Wright, G. J. *Tetrahedron* **1970**, *26*, 1311. Coxon, J. M.; Hartshorn, M. P.; Sutherland, B. L. S. *Aust. J. Chem.* **1974**, *27*, 679. The epimeric 6-*tert*-butyl-1-oxaspior[2,5]octanes react with ^{18}O-labeled acetone to give epimeric mixtures of dioxolanes with the ^{18}O attached to the cyclohexyl ring, consistent with a preference for axial attack of an intermediate tertiary cation coupled with a preference of acetone attack with inversion. The formation of dioxolane by reaction of the aldehydes **3** and **4** with epoxides **2** or **1** introduces a correction due to the secondary isotope effect for that reaction. The magnitude of this secondary isotope effect is not known, but the relative values of k, k_H, and k_D were evaluated for reasonable values of the isotope effect.[1]

(4) Coxon, J. M.; Hartshorn, M. P.; Sutherland, B. L. S. *Tetrahedron Lett.* **1969**, 4029. Blackett, B. N.; Coxon, J. M.; Hartshorn, M. P.; Richards, K. E. *Tetrahedron* **1969**, *25*, 4999. Coxon, J. M.; Hartshorn, M. P.; Muir, C. N. *Tetrahedron* **1969**, *25*, 3925 and references therein. Blackett, B. N.; Coxon, J. M.; Hartshorn, M. P.; Jackson, B. L. J.; Muir, C. N. *Tetrahedron* **1969**, *25*, 1479.

10.1021/jo000591b CCC: $19.00 © 2000 American Chemical Society
Published on Web 11/10/2000

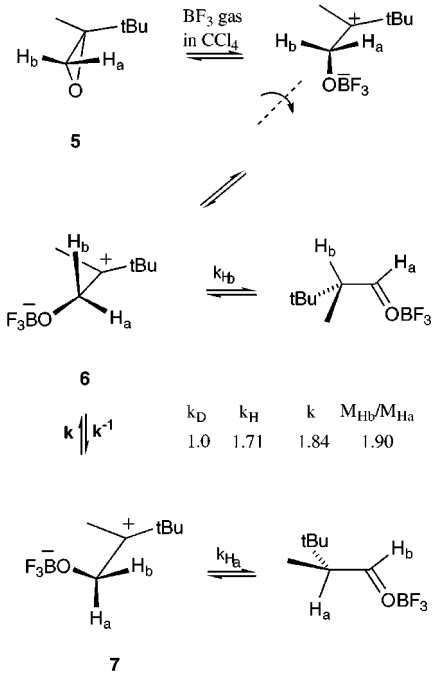

Figure 2. Mechanism for the rearrangement of 2,3,3-trimethyl-1,2-epoxybutane.

latter conformer and H_b from the former. The origin of the stereoselectivity therefore lies in the relative magnitude of the rate constants, k ($=k^{-1}$) and k_{H_a} ($=k_{H_b}$), which if they are comparable[5] or if hydride migration is fast relative to conformational change of the cation (**6** ↔ **7**) results in a bias in favor of H_b migration. In both these situations, H_b migration is favored because conformation **6**, from which H_b migration occurs, is formed before the structure undergoes conformational change to **7**. Alternatively, if hydride migration were slow relative to the conformational change ($k_H \ll k$ ($= k^{-1}$)), no stereoselection would be observed. On the basis of this mechanistic model[6] and substitution of the results of the product analysis from the rearrangement of epoxides **1** and **2**, the relative values of the rate constants with $k_D = 1.0$[1] were established as $k_H = 1.73$ and the rate of conformational change for **6** ↔ **7** as $k = 1.83$.[7] For the undeuterated epoxide **5** (where $H_a = H_b = H$), the data allow the estimation for the preferential migration of the hydrogen atom cis to the methyl group (i.e., M_{H_b}/M_{H_a} in the range of 1.81−1.93:1). The range in the value accommodates a small unknown secondary isotope effect in the reaction of the CHO and CDO with epoxide to give dioxolane.[1]

In a computational study of the rearrangement of BF_3-coordinated methylpropene oxide to BF_3-coordinated methyl propanal involving a 1,2-hydride shift, two possible conformations of an intermediate carbocation with the BF_3 group either in or below the plane of the carbon framework were identified.[8] Theoretical primary and secondary isotope effects were calculated and were consistent with an "early" transition structure for hydride migration. A comparison is drawn between these results and those of the present study. We now report a theoretical study, using ab initio and density functional methods, of the rearrangement of BF_3-coordinated 2,3,3-trimethyl-1,2-epoxybutane, including the calculation of kinetic isotope effects, to establish if theory provides a potential energy surface consistent with the experimental results.

Computational Methods

Exploratory calculations of the potential energy surface were carried out at the semiempirical AM1 level[9] followed by ab initio calculations at the HF/6-31G* level. Electron correlation was accounted for through the use of the gradient-corrected hybrid density functional DFT(B3LYP)/6-31G* theory.[10] Intrinsic reaction coordinate (IRC) calculations at the B3LYP/6-31G* level were used to establish the relevance of the transition structures with respect to the minima on the potential energy surface. Vibrational frequencies were computed at 298.15 K and scaled by 0.961 for the B3LYP/6-31G* optimized structures accordingly.[11] Single-point solvation calculations were performed on the gas-phase B3LYP/6-31G* optimized stationary points at the same level of theory in conjunction with the self-consistent isodensity polarized continuum model[12] SCRF(SCI-PCM) within Gaussian 94.[13] A dielectric constant of 2.23[14] was used, representing CCl_4. The zero-point-corrected stationary point energies are reported in Table 1.

Theoretical primary and secondary kinetic isotope effects were calculated for the stationary points of interest using methodology derived by Bigeleisen and Mayer and based on the principles of statistical mechanics and transition-state theory.[15] For the calculation of kinetic isotope effects, Bigeleisen and Mayer[16] derived an equation[17] for k_H/k_D which, in the absence of symmetry number effects, contains only terms for all the vibrational

(5) Such comparability of rates has been noted in other carbonium ion studies: Collins, C. J.; Bonner, W. A.; Lester, C. T. *J. Am. Chem. Soc.* **1959**, *81*, 466. Collins, C. J.; Benjamin, B. N. *J. Am. Chem. Soc.* **1963**, *85*, 2519.

(6) The possibility of the reversible collapse of conformer **6** to epoxide and the analogous collapse of conformer **7** to the epimeric epoxide does not invalidate the results derived using this simplified model.

(7) The expressions used were **4**/**3** = 1/0.89 = $(k_D/k_H)[1 + (k_H/k)]$ and **3**/**4** = 2.65 = $k_H/k_D[1 + (k_D/k)]$.

(8) Coxon, J. M.; Thorpe, A. J.; Smith, W. B. *J. Org. Chem.* **1999**, *64*, 9575.

(9) Dewar, M. J. S.; Zoebisch, E. G.; Healy, E. F.; Stewart, J. J. P. *J. Am. Chem. Soc.* **1985**, *107*, 3902.

(10) Becke, A. D. *Phys. Rev. A* **1988**, *38*, 3098. Becke, A. D. *J. Chem. Phys.* **1993**, *98*, 1372. Lee, C.; Yang, W.; Parr, R. G. *Phys. Rev. B* **1988**, *37*, 785.

(11) Foresman, J. B.; Frisch, Æ. *Exploring Chemistry with Electronic Structure Methods*, 2nd ed.; Gaussian, Inc.: Pittsburgh, PA, 1996; Chapter 4, p 62.

(12) Foresman, J. B.; Keith, T. A.; Wiberg, K. B.; Snoonian, J.; Frisch, M. J. *J. Phys. Chem.* **1996**, *100*, 16098.

(13) Frisch, M. J.; Trucks, G. W.; Schlegel, H. B.; Gill, P. M. W.; Johnson, B. G.; Robb, M. A.; Cheeseman, J. R.; Keith, T.; Petersson, G. A.; Montgomery, J. A.; Raghavachari, K.; Al-Laham, M. A.; Zakrzewski, V. G.; Ortiz, J. V.; Foresman, J. B.; Cioslowski, J.; Stefanov, B. B.; Nanayakkara, A.; Challacombe, M.; Peng, C. Y.; Ayala, P. Y.; Chen, W.; Wong, M. W.; Andres, J. L.; Replogle, E. S.; Gomperts, R.; Martin, R. L.; Fox, D. J.; Binkley, J. S.; Defrees, D. J.; Baker, J.; Stewart, J. P.; Head-Gordon, M.; Gonzalez, C.; Pople, J. A. *Gaussian 94*, revision D.2; Gaussian, Inc.: Pittsburgh, PA, 1995.

(14) *Handbook of Chemistry and Physics*, 60th ed.; Weast, R. C., Ed.; CRC Press: Boca Raton, FL, 1980; p E55.

(15) Isotope effects are considered to arise from a contribution of individual partition functions representing translational, rotational, electronic, and vibrational energy levels, represented by $k_h/k_d = Q_{trans}Q_{rot}Q_{elec}Q_{vib}$ where Q is expressed as $Q = \sum p_i e_i^{-ei/KT}$.

(16) Bigeleisen, J.; Mayer, M. G. *J. Chem. Phys.* **1947**, *15*, 261. Bigeleisen, J. *J. Chem. Phys.* **1949**, *17*, 675. Bigeleisen, J.; Wolfsberg, M. *Adv. Chem. Phys.* **1958**, *1*, 15.

(17) The subscripts 1 and 2 refer to the atomic masses of hydrogen and deuterium, respectively, and u_i is defined by the following parameters: a normal-mode harmonic frequency v_i, the Boltzmann constant k, and the absolute temperature T in K. The reactant molecule is represented by $3N - 6$ normal vibrational modes where N is the number of atoms in the molecule. For transition structures, there are $3N - 7$ normal vibrational modes because the imaginary frequency is not treated as a proper vibrational mode and any movement away from the saddle point results in decomposition along the reaction coordinate.

Table 1. Energies of Stationary Points[a]

	optimized	energy (au)	ZPVE (au)	energy + scaled ZPVE (au)	imaginary frequencies (i cm^{-1})	energy relative to minimum **8** (kcal/mol)
			Transition Structures			
12	B3LYP/6-31G*	−674.90517	0.21269	−674.70078	160.6	+21.0
	B3LYP/6-31G* (SCI-PCM)	−674.91431[b]				+19.0
11	B3LYP/6-31G*	−674.88935	0.21118	−674.68641	126.6	+30.1
	B3LYP/6-31G* (SCI-PCM)	−674.90214				+26.7
10	B3LYP/6-31G*	−674.89386	0.21110	−674.69100	74.2	+27.2
	B3LYP/6-31G* (SCI-PCM)	−674.90813[b]				+22.9
17	B3LYP/6-31G*	−674.89727	0.20964	−674.69581	24.8	+24.2
	B3LYP/6-31G* (SCI-PCM)	−674.91285[b]				+20.0
18	B3LYP/6-31G*	−674.89849	0.20949	-674.69718	664.6	+23.3
	B3LYP/6-31G* (SCI-PCM)	−674.90979[b]				+21.9
19	B3LYP/6-31G*	−674.89922	0.20957	−674.69783	330.7	+22.9
	B3LYP/6-31G* (SCI-PCM)	−674.91228[b]				+20.3
			Minima			
8	B3LYP/6-31G*	−674.94005	0.21410	-674.73430		0.0
	B3LYP/6-31G* (SCI-PCM)	-674.94464[b]				0.0
9	B3LYP/6-31G*	-674.93464	0.21385	-674.72914		+3.2
	B3LYP/6-31G* (SCI-PCM)	−674.93837				+3.9
15	B3LYP/6-31G*	-674.90239	0.210425	-674.70018		+21.4
	B3LYP/6-31G* (SCI-PCM)	−674.91605[b]				+17.9
16	B3LYP/6-31G*	-674.90368	0.21107	-674.70085		+21.0
	B3LYP/6-31G* (SCI-PCM)	-674.916097[b]				+17.9
14	B3LYP/6-31G*	-674.96777	0.21344	-674.76266		−17.8
	B3LYP/6-31G* (SCI-PCM)	−674.97339[b]				

[a] ZPVE scaled by 0.961 (B3LYP). [b] B3LYP/6-31G* (SCI-PCM) single-point calculations with a dielectric constant of 2.23 (CCl_4) at 298.15 K.

frequencies of the reactant and transition structure. They showed that in most cases the contribution to the overall isotope effect by the translational, rotational, and electronic partition functions[15] is negligible and can be ignored.

The kinetic isotope effect is expressed as the ratio of the reduced isotopic partition function of the reactant $(S_2/S_1)f_{react}$ divided by the reduced isotopic partition

$$u_i = hv_i/kT = 1.4387v_i/T$$

$$\left(\frac{S_2}{S_1}\right)f_{react} = \prod_i^{3N-6} \frac{u_{2i}}{u_{1i}} \frac{[1 - e^{-u_{1i}}]}{[1 - e^{-u_{2i}}]} \exp\left[\sum_i^{3N-6} \frac{(u_{1i} - u_{2i})}{2}\right]$$

$$\left(\frac{S_2}{S_1}\right)f_{TS} = \frac{V_{1L}\dagger}{V_{2L}\dagger} \prod_i^{3N-7} \frac{u_{2i}}{u_{1i}} \frac{[1 - e^{-u_{1i}}]}{[1 - e^{-u_{2i}}]} \exp\left[\sum_i^{3N-7} \frac{(u_{1i} - u_{2i})}{2}\right]$$

$$\frac{k_H}{k_D} = \frac{(S_2/S_1)f_{react}}{(S_2/S_1)f_{TS}}$$

function of the transition structure $(S_2/S_1)f_{TS}$, the latter of which includes a term $(V_{1L}\dagger/V_{2L}\dagger)$ representing the ratio of imaginary frequencies of the nondeuterated and deuterated transition structures.

The data used to calculate the isotope effects was obtained from the output of Gaussian frequency calculations on the B3LYP/6-31G* optimized stationary points,[18] which yield individual vibrational frequencies and Gibbs free energy values.[19] In a similar study[8] involving 1,2-hydride shifts, tunneling effect corrections were calculated and shown to result in no significant change in the magnitude of primary and secondary isotope effects. For the present study, no account of tunneling effect corrections to the theoretically calculated isotope effects has therefore been made.

Results and Discussion

Complex formation of BF_3 and 2,3,3-trimethyl-1,2-epoxybutane can occur on either face of the epoxide, resulting in the formation of the stationary points **8** and **9** (Figure 3). Structure **8** with BF_3 coordinated to the less-hindered epoxide face syn to the methyl is 3.3 kcal/mol lower in energy than the anti invertomer[20] **9**. This is a consequence of the greater steric interaction between the BF_3 and the bulky *tert*-butyl group in the latter than between the BF_3 and the methyl in the former. The preference for ring opening to occur at the more stable tertiary C2 center of **8** and **9** is reflected in a longer C2−O bond in **8** (1.490 Å) and **9** (1.489 Å) relative to the corresponding C1−O bonds (1.454 Å in **8** and 1.444 Å in **9**).

Ring opening of **8** can occur by transition structure **10** where H_a is favorably aligned for migration with the carbocation (H_a−C1−C2−C3 = 75.6°) and already exhibits some hyperconjugation with C2. C1−H_a is longer (1.112 Å) and the H_a−C1−C2 bond angle (107.4°) is

(18) Cautionary comment: We have found that if a scale factor of 1.0 is not specified in the Gaussian program input file for an isotope calculation, the program automatically assigns a scale factor of 0.8929. If the original frequency data (from which the checkpoint file is used for an isotope calculation) is not scaled and is used in conjunction with the isotope calculation frequency data, erroneous values for isotope effects will result.

(19) The isotope effects can also be calculated using the following equation which utilizes the difference in Gibbs free energy (G) between the nondeuterated and deuterated reactant and transition structures. $k_H/k_D = e^{-(\Delta G_H - \Delta G_D)/RT}$ where $\Delta G = G\dagger - G^r$ with † = transition structure and r = reactant. The required data is also tabulated in the standard output of a Gaussian frequency calculation. Although the Bigeleisen−Mayer equation requires more input data than the equation above, we have chosen to use the former, in which individual frequencies from the Gaussian output are used, in order to gain a better understanding of the vibrational frequencies which most influence the overall isotope effect.

(20) The term "invertomer" has been coined to describe the diastereomers resulting from positioning of a proton on either face of an epoxide. George, P.; Bock, C. W.; Glusker, J. P. *J. Phys. Chem.* **1990**, *94*, 8161.

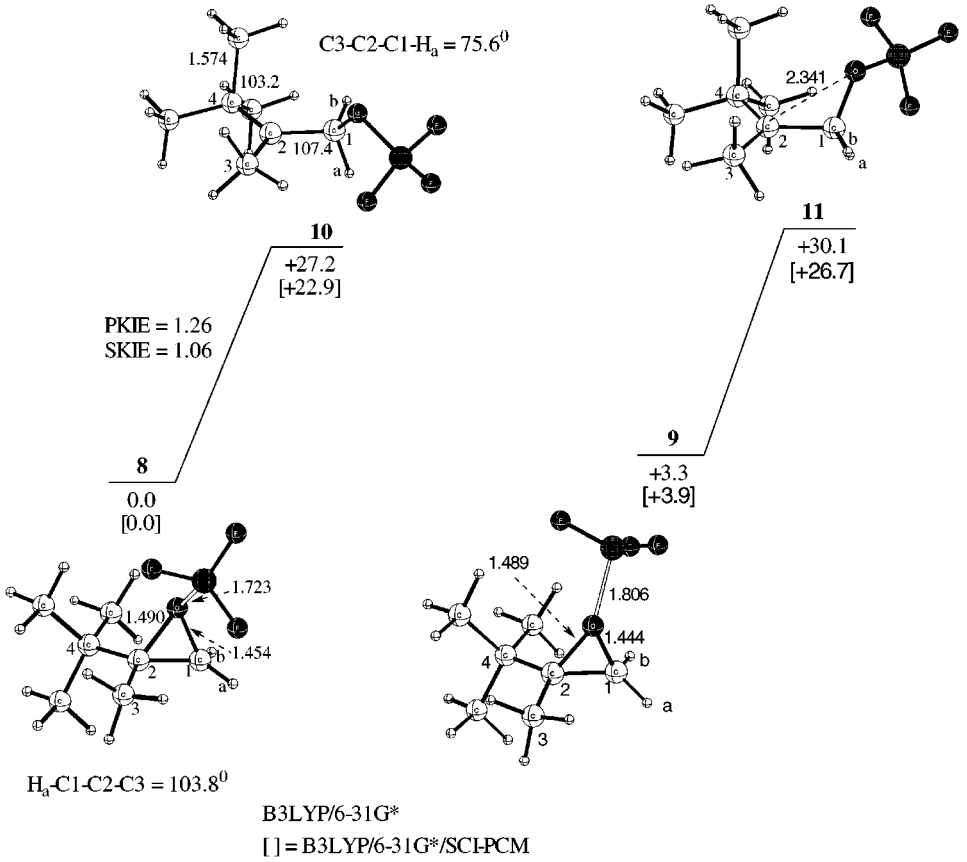

Figure 3. Ring opening for syn and anti BF_3-coordinated 2,3,3-trimethyl-1,2-epoxybutane, **8** and **9**, via transition structures **10** and **11**.

somewhat tighter than the corresponding values (1.086 Å and 109.5°) for **8**. An IRC calculation on **10** led in one reaction coordinate direction to **8** but did not successfully converge to a minimum in the other direction. Single-point solvent calculations lowered the gas-phase energy of **10** (+27.2 kcal/mol) by 4.3 kcal/mol to 22.9 kcal/mol relative to **8** (Figure 3).

For the higher energy invertomer **9**, where BF_3 is coordinated syn to the *tert*-butyl, a transition structure, **11**, was identified for ring opening at C2 which is 26.8 kcal/mol higher in energy than **9** (Figure 3). Lengthening of the C2−O bond is accompanied by rotation of the $O-BF_3^-$ group about C1−C2 and away from the methyl group and results in an interaction between the OBF_3^- and *tert*-butyl. In this conformation, the $C1-H_b$ is almost aligned with the C2 cation p-orbital and is in a favorable position to migrate to C2. The potential energy surface for the ring opening process involving **9** and **11** was not investigated further because of the higher energy of **9** (+3.3 kcal/mol) relative to **8** and confirms the premise[1] that ring opening occurs with the OBF_3 group rotation away from the *tert*-butyl.

The lowest energy transition structure, **12**, identified on the potential energy surface for reaction of epoxide **5** with BF_3, shows ring opening accompanied by rotation about C1−C2 to position a fluorine (C2−F = 2.556 Å) for intramolecular reaction with the carbocation at C2 with retention of configuration (Figure 4). At the transition structure **12**, neither H_a or H_b is positioned to migrate (O−C1−C2−C4 = 133.9°). An IRC calculation on **12** went to completion in both reaction coordinate directions to give **8** and **13**, the latter involving migration of fluorine from the BF_3 group to C2. Fluorohydrin, which would be the product of workup of such a reaction, is not observed in the experiment.[21] Because **13** is a weaker Lewis acid than BF_3 and because of the absence of >1 mol equiv of BF_3, rearrangement to aldehyde would not be expected because **13** is unlikely to act as a Lewis acid catalyst for the removal of the C2−F. The reaction **8** → **13** is exothermic and is not expected to be reversible. Therefore, the fluoro compound **13** does not appear to be on the potential energy surface to aldehyde. Single-point SCRF(SCI-PCM) solvent calculations on the B3LYP/6-31G* optimized geometries lowered the electronic energy barrier between **8** and **12** by 2 kcal/mol.

We have investigated the ring opening of **8** via transition structure **10** extensively in order to establish in as much detail as possible the nature of the potential energy surface leading to aldehyde (Figure 5). In particular, we sought to determine whether the computational methods employed showed the 1,2-hydride/deuteride migration to aldehyde occurred via a concerted process or by a two-step mechanism requiring the intermediacy of a carbocation.

Two carbocation intermediate conformers, **15**[22] and **16**, which are of comparable energy were identified on the

(21) Fluorohydrins have been reported for reaction of epoxides with BF_3 in ether and are known to rearrange on further reaction with BF_3.[4] Coxon, J. M.; Hartshorn, M. P.; Lewis, A. J.; Richards, K. E.; Swallow, W. H. *Tetrahedron* **1969**, *25*, 4445. Coxon, J. M.; Lawrey, M. G. *Chem. Ind.* **1969**, 1558.

(22) Structure **15** did not fully converge to a minimum, however the optimization calculation ran a number of steps with converged maximum and rms force constants and with no further change in energy. A frequency calculation on **15** yielded all positive vibrational frequencies, and because of the lack of imaginary frequencies, this structure is assumed to be an energy minimum.

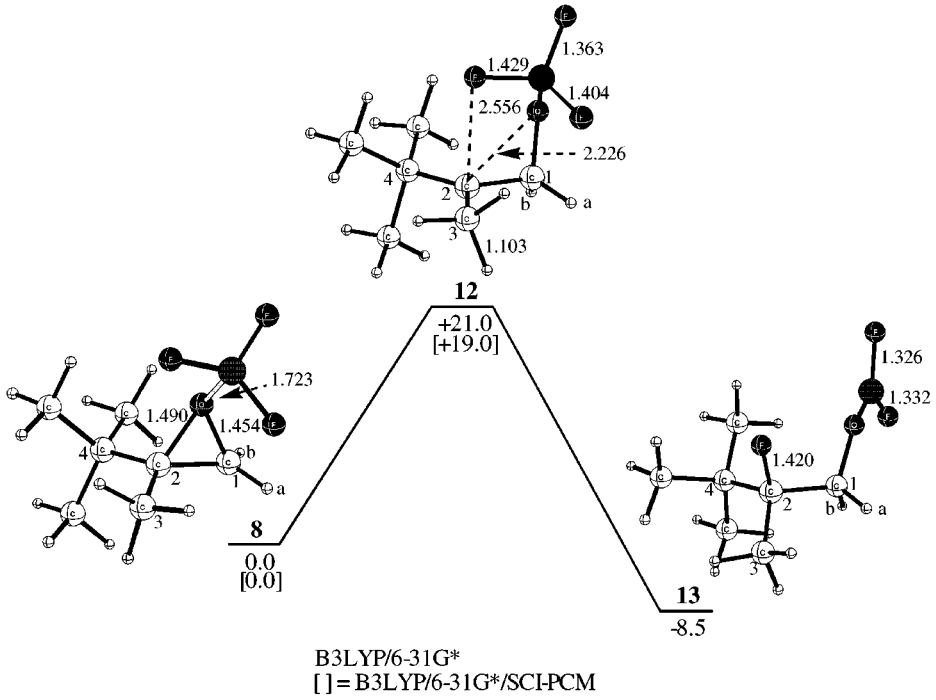

Figure 4. The addition of BF_3 to 2,3,3-trimethyl-1,2-epoxybutane. All stationary points are optimized at the B3LYP/6-31G* level. Bond lengths are in Å with energies relative to **8** in kcal/mol.

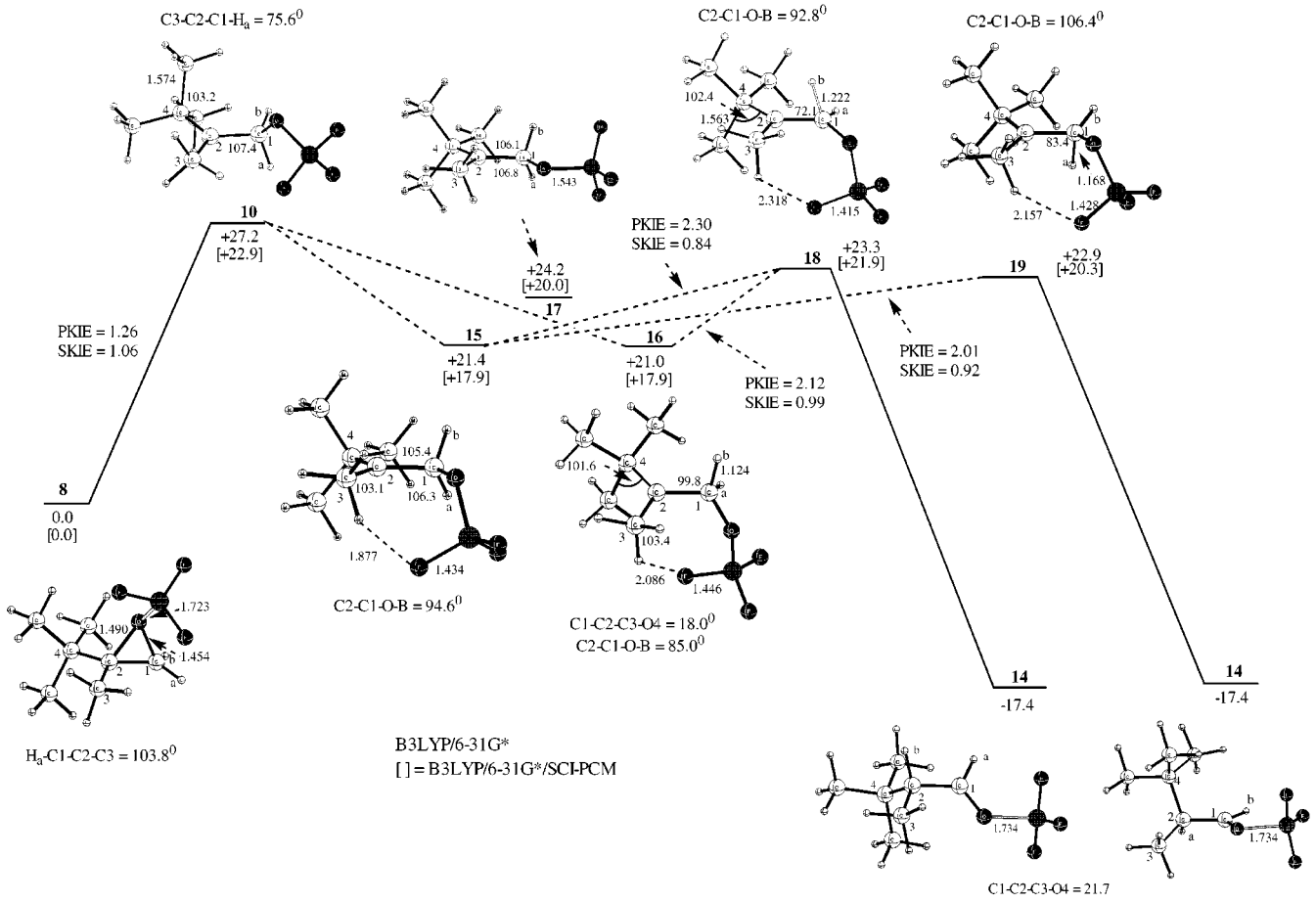

Figure 5. The potential energy surface for the rearrangement of BF_3-coordinated 2,3,3-trimethyl-1,2-epoxybutane **8** to BF_3-coordinated aldehyde **14**. All stationary points are optimized at the B3LYP/6-31G* level. Bond lengths are in Å with energies relative to the complex **8** of epoxide with BF_3 in kcal/mol.

potential energy surface. The former is 0.4 kcal/mol higher in energy than **16** in the gas phase and is equivalent in energy with the solvent. Conformer **15** is assumed to result from rotation of the O−BF_3^- in **10**

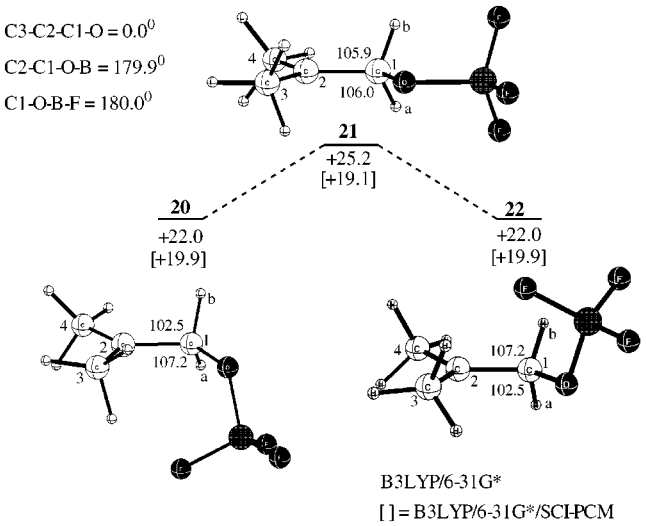

Figure 6. Conformations of cation from ring opening of methylpropene oxide with BF_3.

toward the methyl, resulting in a nearly planar O1−C1−C2−C3 torsion angle. In this conformation, both H_a and H_b show hyperconjugation with the C2 cation and are equally favored to undergo a 1,2-hydride shift with either inversion or retention of configuration, respectively. Conformations **15** and **16** are assumed[1] to interconvert by rotation of the O−BF_3 about the C1−C2 bond along with rotation of the *tert*-butyl group. In conformation **16**, C1−H_b is almost aligned with the p-orbital of the cation whereas C1−H_a is nearly eclipsed with C2−C4 and is therefore not positioned to migrate. The *tert*-butyl group in **16** has rotated from its orientation in **15**, and a hydrogen of the methyl group, anti with respect to the C1−H_b, exhibits hyperconjugation with the cation. An alternative rotation that also brings about the transformation of **10** to the mirror image of **16** but without rotation of the *tert*-butyl involves rotation of the OBF_3^- about the C1−O bond; however, this is considered to be a higher energy process.

In our attempt to find a carbocation intermediate minimum with the O−BF_3^- group in the C2−C1−O plane, we located a transition structure, **17** (Figure 5), 24.2 kcal/mol higher in energy than **8**. This transition structure is different from others on the potential energy surface in that the O−B bond is in the O−C1−C2 plane and the O−C1 bond is in the C1−C2−C3 plane (C3−C2−C1−O is 0° and C2−C1−O−B is 179.9°). A frequency calculation revealed the presence of a small single imaginary frequency (24i cm^{-1}), and animation of this frequency showed the BF_3 to be "wagging" above and below the C2−C1−O plane. An IRC calculation failed to progress significantly in either reaction coordinate direction, and as such the relevance of **17** to the other stationary points on the potential energy surface is not clear.

A transition structure, **21**, similar to **17** was identified at the B3LYP/6-31G* level in a previous study[8] of the BF_3-catalyzed rearrangement of methylpropene oxide (Figure 6). In that study, **21** was identified as a transition structure in the gas phase for interconversion between carbocation conformer **20** with the O−BF_3^- group lying below the C2−C1−O plane and its mirror image **22** with the O−BF_3^- above the plane. Single-point solvent calculations lowered the energy of **21** to below that of **20**. The transition structure **21**, with both H_a and H_b equally positioned to migrate, was assumed to be a valid minimum in solvent from which a 1,2-hydride/deuteride migration could occur. However, in the present study a single-point solvent calculation on **17** (Figure 5) did not give an energy lower than the single-point solvent energies of **15** and **16**. We therefore consider **17** not to be a significant intermediate to facilitate a 1,2-hydride shift on the potential energy surface.

Two transition structures, **18** and **19**, for hydride migration between C1 and C2 were identified on the potential energy surface (Figure 5). IRC calculations on each progressed to completion in one reaction coordinate direction to give enantiomers of the BF_3−aldehyde complex **14**. The calculations did not progress to any significant extent in the reverse reaction coordinate direction because of convergence failure close to the transition structures. The potential energy surface is considered to be relatively flat in this region. Both **18** and **19** show considerable structural similarity[23] with intermediates **16** and **15**, with the BF_3 group below the C3−C2−C1−O plane in all four structures. Because of this structural similarity, the potential energy surface is assumed to connect **16** with **18** (H_b-migration) and **15** with both **18** (H_b-migration) and **19** (H_a-migration) (Figure 5). The latter transition structure is marginally lower in energy by 0.4 kcal/mol in the gas phase and by 1.6 kcal/mol with single-point solvation calculations.

For the lower energy transition structure **19**, the H_a−C1−C2 bond angle (83.4°) is tighter and C1−H_a (1.168 Å) is longer than in **15** (106.3° and 1.114 Å). The small energy difference (1.5 kcal/mol in the gas phase and 2.4 kcal/mol with solvent) between **15** and **19** is consistent with an early transition structure in accord with the Hammond principle.[24] Interaction of a C3−H with a fluorine is maintained in **19** (C3−H−F = 2.157 Å), although it is weaker than that in **15** (1.877 Å). Hydride migration via **18** is somewhat more advanced than in **19**, as shown by a more contracted C2−C1−H_b bond angle (72.1°) and a longer C1−H_b bond (1.222 Å). There is less interaction between a fluorine of the BF_3 group and a C3 hydrogen in **18** (C3−H−F = 2.318 Å) than in **16** (C3−H−F = 2.086 Å) or **15** (C3−H−F = 1.877 Å).

Analysis of the Calculated Theoretical Kinetic Isotope Effects

Kinetic isotope effects (KIEs),[25] which reflect changes in reaction rate as a result of isotopic substitution and

(23) For **18** and **19**, the OBF_3 has rotated about C1−O (C2−C1−O−B = 92.8° for **18** and 106.40° for **19**) in opposite directions relative to its positions in **15** (C2−C1−O−B = 85.00°) and in **16** (C2−C1−O−B = 94.60°).

(24) Hammond, G. S. *J. Am. Chem. Soc.* **1955**, *77*, 334.

(25) Kinetic isotope effects, expressed as the ratio k_H/k_D, are termed "normal" if $k_H/k_D > 1$ and inverse when $k_H/k_D < 1$. When the bond to an isotope is broken during the course of a reaction, a primary kinetic isotope effect (PKIE) is observed for that step in the reaction process. The magnitude of the PKIE is determined largely from differences between the C1−H(D) stretching frequencies between the reactant and the transition structure, which decrease upon isotopic substitution. Secondary kinetic isotope effects (SKIEs) arise when the bond to the isotope is at the reaction center but is not broken during the course of a reaction. The isotope influences nearby vibrations. Changes in the C_α−H(D) out-of-plane bending frequencies are the most important in effecting the SKIE. Streitweiser, A., Jr.; Jagow, R. H.; Fahey, R. C.; Suzuki, S. *J. Am. Chem. Soc.* **1958**, *80*, 2326. More recent work has shown that changes in stretching as well as bending vibrations can be important in SKIEs. Zhao, X. G.; Tucker, S. C.; Truhlar, D. G. *J. Am. Chem. Soc.* **1991**, *113*, 826. Zhao, X. G.; Lu, D.-H.; Liu, Y.-P.; Lynch, D. G.; Truhlar, D. G. *J. Chem. Phys.* **1992**, *97*, 6369.

Table 2. Vibrational Multiplicative Contributions to the Total Kinetic Isotope Effects for 1,2-Hydride Migration at 298 K

	KIE	$\nu < 750$ cm^{-1}	$750 < \nu <$ 2000 cm^{-1}	$\nu > 2000$ cm^{-1}	($\nu_D^\dagger/\nu_H^\dagger$)
15 → 19	PKIE = 2.012	1.026	1.214	1.288	1.255
	SKIE = 0.916	1.040	0.886	0.914	1.089
15 → 18	PKIE = 2.304	1.031	1.166	1.543	1.242
	SKIE = 0.843	1.011	0.901	0.899	1.029
16 → 18	PKIE = 2.125	1.057	1.093	1.482	1.242
	SKIE = 0.985	1.001	0.995	0.961	1.029

are related to structural changes between reactant and transition structure, can be used to provide mechanistic information.[26] The vibrational modes in which there is a significant change between the reactant and transition structure contribute most to the KIE. The calculated primary and secondary kinetic isotope effects are presented in Figure 5 and Table 2. Included in Table 2 are the multiplicative contributions determined from the nondeuterated and deuterated vibrational frequencies, which collectively give rise to each isotope effect. The vibrational frequencies are broadly classified into three categories: a low-frequency group ($\nu < 750$ cm^{-1}) relating to out-of-plane bending frequencies and all modes unique to the transition structures in which there are no corresponding vibrations in the reactant, a middle-frequency group ($750 < \nu < 2000$ cm^{-1}) representing in-plane and out-of-plane bending modes, and a high-frequency group ($\nu > 2000$ cm^{-1}) corresponding to stretching vibrations. The latter two categories generally provide the greatest contribution to the size of the isotope effect. Ring opening of **8** via transition structure **10** is the rate-determining step for the molecular rearrangement on the potential energy surface. This transition structure is calculated to be higher in energy than transition structures **18** and **19** by 3.9 and 4.3 kcal/mol in the gas phase and by 1.0 and 1.6 kcal/mol in solvent, respectively. No evidence could be found that **10** rearranges in a concerted process to aldehyde. A small primary kinetic isotope effect (PKIE) calculated between **8** and **10** ($k_H/k_D = 1.26$, cf. experimental value 1.71), along with the absence of significant hyperconjugation of the C1−H_a with C2 at the transition structure **10** even though C1−H_a is almost in the plane of the C2 carbocation, mitigates against transition structure **10** being on a concerted pathway from **1** to aldehyde. An IRC calculation on **10** in the forward reaction coordinate direction failed to converge to aldehyde or in fact to cation.

Hydride migration between C1 and C2 from intermediate **16** is favored to occur via **18** because C1−H_b is more appropriately aligned with the C2 p-orbital than C1−H_a (Figure 5). The size of the calculated PKIE ($k_H/k_D = 2.12$) for C1−H_b migration (**16** → **18**) is consistent with the marked reduction in the C2−C1−H_b bond angle (99.8° for **16** → 72.1° for **18**) and lengthening of the C1−H_b bond (1.124 Å for **16** → 1.222 Å for **18**) in going to the transition structure.[27] This isotope effect is predominantly a consequence of the difference between the nondeuterated and deuterated stretching frequencies (>2000 cm^{-1}) of **16** being greater than the corresponding diffference for **18**.

A very small inverse secondary kinetic isotope effect (SKIE) is calculated ($k_H/k_D = 0.99$) for the migration of H_b when C1−H_a is replaced with deuterium, consistent with the very small difference between the nondeuterated and deuterated bending frequencies ($750 < \nu < 2000$ cm^{-1}) of **16** compared to the analogous modes of **18**.

For intermediate **15**, the relative positioning of H_a and H_b with respect to the carbocation p-orbital is such that both should be comparably favored to undergo migration. The orientation of the OBF_3^- is, however, not positioned symmetrically with respect to H_a and H_b, and for the preferred pathway involving H_a migration, the OB bond is nearly planar with C−H_a. Migration of the H_b from **15** is expected to occur via transition structure **18**, and a PKIE for this step was calculated as $k_H/k_D = 2.30$. For transition structure **18**, the migrating proton is positioned close to midway between C1 and C2, and this compares to an earlier transition structure for H_a migration via **19**.

A large inverse kinetic secondary isotope effect[28] was calculated ($k_H/k_D = 0.84$) for the hydride/deuteride shift between **15** → **18**. A hybridization change from sp^3 in a reactant to sp^2 at a transition structure is generally observed to give rise to a normal isotope effect. The inverse nature of the SKIE isotope effect between **15** → **18** is therefore surprising. This is attributed to the difference between the nondeuterated and deuterated bending frequencies of **18** being greater than the corresponding diffference for **15**, resulting in an inverse contribution (0.901) to the isotope effect (Table 2).

From intermediate **15**, the lower energy pathway to aldehyde **14** involves migration of H_a via **19**, which is 0.4 and 1.5 kcal/mol lower in energy in the gas and solvent phases, respectively, than H_b migration via **18**. A smaller PKIE was calculated for **15** → **19** ($k_H/k_D = 2.01$) than for **15** → **18** ($k_H/k_D = 2.30$), reflecting the fact that hydride migration is less advanced in the former process (C2−C1−H_a = 83.4° for **19** vs C2−C1−H_b = 72.1° for **18**). The largest contribution to the overall PKIE between **15** and **19** is from the high stretching frequencies (>2000 cm^{-1}) and from the midrange bending frequencies ($750 < \nu < 2000$ cm^{-1}), with multiplicative contributions of 1.288 and 1.214, respectively (Table 2).

A large inverse SKIE was calculated ($k_H/k_D = 0.92$) for **15** → **19**. Its magnitude reflects tighter bonding at C1 in the transition structure than in **15**, with the difference between the nondeuterated and deuterated bending and stretching frequencies of **19** being greater than the corresponding difference for **15**. The individual frequencies responsible for the observed SKIE were examined in more detail.[29] A large normal contribution to the SKIE is provided by the larger difference between the C1−H_b (2839 cm^{-1}) and C1−D_b (2109 cm^{-1}) stretching frequencies of intermediate **15** compared to the difference between the stretching frequencies C1−H_b (3022 cm^{-1}) and C1−D_b (2469 cm^{-1}) of **19**. This is, however, counter-

(26) Melander, L. *Isotope Effects on Reaction Rates*; Ronald Press Co.: New York, 1960.

(27) Experimentally determined deuterium isotope effects for 1,2-hydride shifts lie in the range of 1.2−3.0. Myhre, P. C.; Brown, K. S. *J. Am. Chem. Soc.* **1969**, *91*, 5639. Myhre, P. C.; Evans, E. *J. Am. Chem. Soc.* **1969**, *91* (1), 5641. Karabatsos, G. J.; Hsi, N.; Meyerson, S. *J. Am. Chem. Soc.* **1970**, *92* (2), 621. Karabatsos, G. J.; Mount, R. A.; Rickter, D. O.; Meyerson, S. *J. Am. Chem. Soc.* **1970**, *92*, 1248.

(28) Isotopically sensitive vibrational modes that increase in frequency in proceeding from the reactant to the transition structure are responsible for inverse SKIEs. Inverse α-deuterium SKIEs are not uncommon for sp^3 → sp^2 processes, and bimolecular S_N2 reactions at methyl have been reported to be as low as 0.87. Llewellyn, J. A.; Robertson, R. E.; Scott, J. W. M. *Can. J. Chem.* **1960**, *38*, 222.

(29) A table of the vibrational frequencies for the nondeuterated and deuterated stationary points **15** and **19** is included with the Supporting Information.

Table 3. Isotope Effect and Relative Rate Data

k_H/k_D	m(real)	m(real)	K_D	K_H	k_{rot}	M_b/M_a
(a) Isotope Effect and Relative Rate Data Estimated by Blackett et al.[a]						
1.00	0.89	2.67	1.0	1.73	1.83	1.94
1.05	0.87	2.55	1.0	1.65	1.82	1.90
1.10	0.85	2.45	1.0	1.53	1.81	1.87
1.15	0.83	2.35	1.0	1.52	1.80	1.84
1.20	0.81	2.26	1.0	1.47	1.80	1.82
(b) Isotope Effect and Relative Rate Data Obtained by Solution of Simultaneous Equations						
1.00	0.89	2.67	1.0	1.73	1.83	1.94
1.05	0.85	2.55	1.0	1.63	1.78	1.92
1.10	0.81	2.45	1.0	1.55	1.72	1.90
1.15	0.78	2.36	1.0	1.47	1.67	1.88
1.20	0.75	2.27	1.0	1.402	1.62	1.87
(c) Correction for a Theoretical Secondary Isotope of 0.916 to Data in Table 3b						
1.00	0.85	2.45	1.0	1.59	1.83	1.87
1.05	0.81	2.34	1.0	1.50	1.77	1.85
1.10	0.78	2.25	1.0	1.42	1.72	1.83
1.15	0.75	2.16	1.0	1.35	1.67	1.81
1.20	0.72	2.08	1.0	1.29	1.61	1.80

[a] Reference 1.

acted by a larger inverse contribution to the overall SKIE from a significant change in the C1−H_a (2468 cm^{-1}) and C1−D_a (2249 cm^{-1}) stretching frequencies of **19**, whereas no significant change is observed for the analogous frequencies in intermediate **15**. The overall effect of the modes with frequencies >2000 cm^{-1} is an inverse multiplicative contribution of 0.914 (Table 2) to the overall isotope effect. The changes in the midrange bending frequencies of nondeuterated **19** (1109 → 1272 cm^{-1}) with isotopic substitution (1057 → 1216 cm^{-1}) are larger than those for intermediate **15** and provide a further significant inverse multiplicative contribution to the SKIE (0.886, Table 2).

The experimental results show that aldehyde formation occurs by preferential stereoselection of C1−H_a, the proton cis to the methyl (Figure 2). M_{H_b}/M_{H_a} is calculated to be in the range of 1.81−1.93:1.[1] The range reflects a small unknown correction (assumed to be between 1 and 1.20) for a secondary isotope effect in the reaction of CHO and CDO with epoxide to form dioxolane. For the mechanistic model (Figure 2), relative values of k_H and k with respect to $k_D = 1$ were similarly established[1] as $k_H = 1.46-1.73$ and $k = 1.83-1.80$ (Table 3a).

For the present study, we have not calculated the SKIE for the reaction of CHO and CDO with epoxide to form dioxolone but expect the value to be small. In a previous paper, we reported an analysis of the variation of the values of k_H and k for the corrections in the range of 1.0−1.2 from the solution of a series of linear equations determined by approximate graphical methods (Table 3a).[1] We now report more accurate solutions to the linear equations, established by the use of the computational program (Maple) designed to solve linear equations (Table 3b).

There is a further correction to be applied to the experimental value of k_H/k_D because this measured value is actually the ratio of the rate constant for H migration from a carbon bonded to deuterium versus deuterium migration from a carbon bonded to hydrogen:

$$\frac{k^{D_{adj}}_{H_{mig}}}{k^{H_{adj}}_{D_{mig}}} = 1.73$$

The true expression for the primary isotope effect is defined as

$$\frac{k^{H_{adj}}_{H_{mig}}}{k^{H_{adj}}_{D_{mig}}}$$

It can be seen that that the experimentally measured ratio needs to be multiplied by a expression for an appropriate secondary isotope effect:

$$\text{SKIE} = \frac{k^{H_{adj}}_{H_{mig}}}{k^{D_{adj}}_{H_{mig}}}$$

to give the required isotope effect:

$$\frac{k^{H_{adj}}_{H_{mig}}}{k^{H_{adj}}_{D_{mig}}} = \frac{k^{D_{adj}}_{H_{mig}}}{k^{H_{adj}}_{D_{mig}}}\,\text{SKIE}$$

The secondary isotope effect was calculated for the lowest energy pathway for hydride migration between **15** and **19** as 0.92. With this correction to the experimentally determined isotope effect (1.73), the required isotope effect is calculated as

$$\frac{k^{H_{adj}}_{H_{mig}}}{k^{H_{adj}}_{D_{mig}}} = 1.73\ \text{SKIE}$$

$$= 1.59$$

The ranges in values of k_H, k, and M_{H_b}/M_{H_a} are presented in Table 3c. The value of the primary isotope effect (1.59) for the lowest energy pathway for hydride migration between **15** and **19** on the potential energy surface compares with the theoretically calculated value of 2.01 (Figure 5).

The isotope effects are sensitive to structure, and the difference in the calculated and experimental values suggests that the structural geometry for the theoretical stationary points differs somewhat from that of the experimental structures. Nevertheless, the structures of the theoretical stationary points provide considerable understanding of the reaction mechanism. Our investigation of the potential energy surface isolated two transition structures, **18** and **19**, and two intermediates, **15** and **16**. There may be other stationary points not characterized. The potential energy surface relating the observed stationary points **10**, **15**, **16**, **18**, and **19** is relatively flat, and the failure of the IRC calculations to run to completion in this flat region of the surface does not allow an interconnectivity of the stationary points to be definitively defined.

If the product aldehyde can be considered to arise exclusively from carbocation intermediate **15**, then applying a standard Boltzmann distribution to the relative electronic gas and solvent phase energies of transition structures **19** and **18** allows the preference for C1−H_a via **19** or C1−H_b via **18** to be established. From **15**, the preference for C1−H_a (via **19**) over C1−H_b (via **18**) is calculated in the gas phase as 1.18:1 and in solvent the value increases to 1.91:1. The latter calculated value of stereoselectivity is remarkably similar to the experimental value of M_{H_b}/M_{H_a} in the range of 1.87−1.80 (Table 3c) in favor of the prochiral hydrogen cis to the methyl.

Incorporating intermediate **16**, in which H_b is positioned to migrate via **18**, into the Boltzmann calculation for C1−H_b and C1−H_a selection reduces the stereoselectivity of H_a from that experimentally observed. We consider that the computational methodology/tools used to search the potential energy surface and to calculate the prochiral selectivity for such a complex system must nevertheless be regarded with caution in the absence of more experimental measurements against which the methodology can be tested.

Conclusion

Gas-phase and SCRF(SCI-PCM) solvent calculations at the B3LYP/6-31G* level of theory support ring opening of 2,3,3-trimethyl-1,2-epoxybutane with BF_3 to 2,3,3-trimethylbutanal via a tertiary carbocation intermediate in conformations **15** and **16** followed by a subsequent step involving hydride migration via transition structures **18** and **19**. The experimentally measured primary isotope effect ($k_H{}^D/k_D{}^H$) requires a correction for an appropriate secondary isotope effect to give a true isotope effect $k_H{}^H/k_D{}^H$. For the lowest energy pathway for hydride migration from **15** to **19**, the calculated SKIE is 0.92. The magnitude of this secondary isotope effect reflects tighter bonding at C1 in transition structure **19** than in **15**, with the difference between the nondeuterated and deuterated bending and stretching frequencies of **19** being greater than the corresponding difference for **15**. This isotope effect applied to the experimentally computed isotope effect ($k_H{}^D/k_D{}^H = 1.47-1.73$) results in a revised primary kinetic isotope effect of $k_H{}^H/k_D{}^H = 1.28-1.59$).

A primary isotope effect was calculated ($k_H{}^H/k_D{}^H = 2.01$) between **15** and **19**, resulting primarily from changes in the C1−H stretching frequencies, and compares with the corrected experimental isotope effect (1.59). The isotope effects are sensitive to structure, and the difference in the calculated and experimental values suggests that the structural geometry for the theoretical stationary points differs somewhat from that of the experimental structures. From intermediate **15**, migration of the C1−H_a proton via **19** is energetically favored over C1−H_b migration via **18** and this result is consistent with the experimental results in which hydride migration of the proton cis to the methyl is favored. The computational methodology/tools available to search the potential energy surface and to calculate the prochiral selectivity for such a complex system must be regarded with caution in the absence of more extensive experimental measurements.

Acknowledgment. We acknowledge grants from the New Zealand Lotteries Board and the Marsden Fund.

Supporting Information Available: Archive material on all stationary points. This material is available free of charge via the Internet at http://pubs.acs.org.

JO000591B